UCRL- 100927
PREPRINT

THE PERIODIC LAW AT HIGH PRESSURES

David A. Young
Lawrence Livermore National Laboratory
University of California
Livermore, CA 94550

This paper was prepared for submittal to the
1989 American Physical Society Topical Conference on
Shock Compression of Condensed Matter
Albuquerque, NM
August 14–17, 1989

August 1989

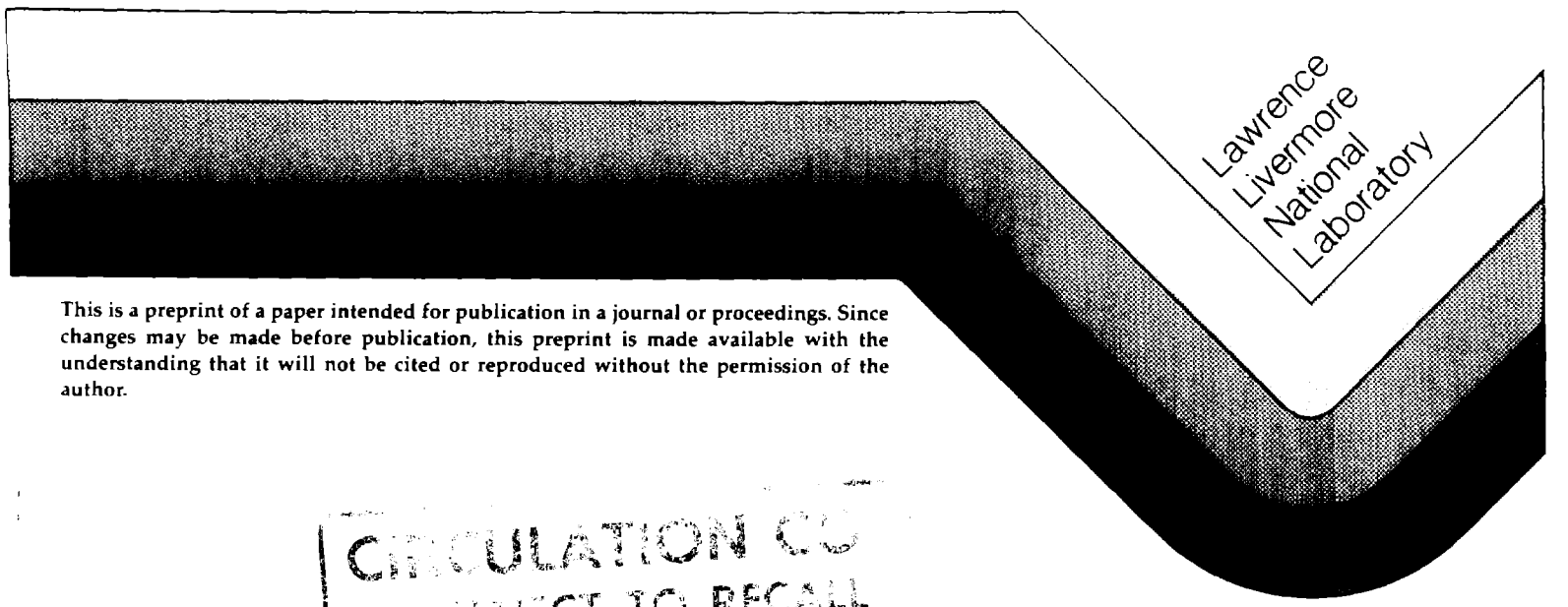

THE PERIODIC LAW AT HIGH PRESSURES

David A. Young

University of California, Lawrence Livermore National Laboratory
Livermore, California 94550, USA

The observed periodicity in the properties of the chemical elements at 1 bar was the basis of the Periodic Table in the 19th century. Modern research on the solid and liquid elements at high pressures and temperatures has revealed new patterns of behavior which provide a deeper understanding of periodicity. These patterns include the rapid convergence of atomic volume with compression to a smooth function of atomic number, the inverse relation between volume and bulk modulus, the waves of crystal structure change which traverse the Periodic Table with increasing pressure, the strong correlation of cohesive energy with melting and critical temperature, and the unusual reordering of melting curves at high pressure. The principle of corresponding states is also related to periodicity and may be generalized.

1. INTRODUCTION

The Periodic Law refers to the recurrence of similar physical and chemical properties as the elements are considered one at a time, with steadily increasing atomic weight. This periodicity has been embodied in more than 100 different forms of the Periodic Table, of which the Long Form is now the most used.[1] Periodicity, now understood in terms of atomic shell structure, is clearly illustrated in a plot of the P = 1 bar atomic volumes (V_o) of the elements vs. atomic weight (A) or number (Z).[2] Lothar Meyer published such a plot as early as 1870, and such correlations of the physical properties of the pure elements contributed importantly to the development of the Periodic Table. In this lecture I will discuss how modern measurements of physical properties of the solid and liquid elements have deepened our understanding of the Periodic Law.

2. EQUATION OF STATE

A modern plot of V_o vs. Z is shown as the upper curve in Fig. 1. Here the four main

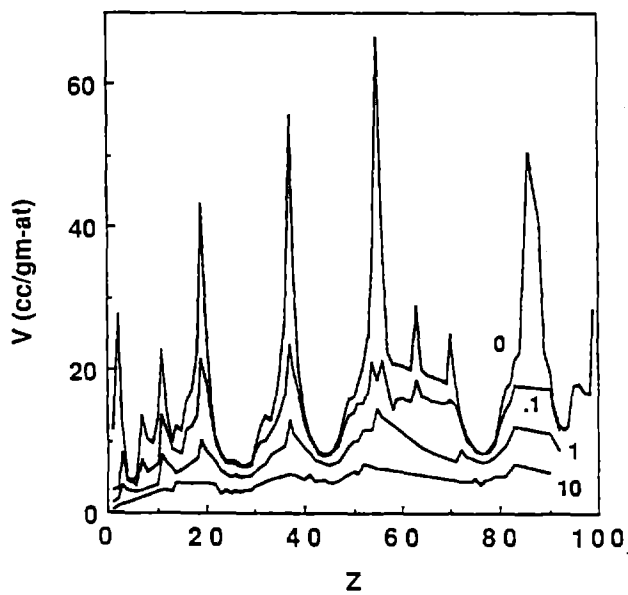

FIGURE 1
The atomic volumes of the elements at four pressures, indicated by the numbers in Mbar.

sharp spikes represent the alkali metals and their neighbor elements. Among the known elements, Cs has the largest atomic volume, and B the smallest. Many new data on the pressure-volume isotherms of the elements have been collected by means of the diamond anvil

*This work was performed under the auspices of the U. S. Department of Energy by LLNL under Contract No. W-7405-Eng-48.

cell in recent years, and we can now make plots of V vs. Z for pressures up to 1 Mbar with good confidence. For higher pressures, theoretical models are needed. The atomic volume is shown in Fig. 1 for pressures of 0, 0.1, 1.0, and 10.0 Mbar. It is remarkable how rapidly the large differences in volume decrease with pressure. By 1 Mbar, the beginnings of a smooth trend may be seen, and this is well-developed by 10 Mbar.[3] Various semiclassical atom models such as the Thomas-Fermi-Dirac come into good agreement with the data at 10 Mbar, as shown in Fig. 2. This shows that the peculiarities of bonding which produce the sharply defined periodic structure in Fig. 1 have been erased by compression.

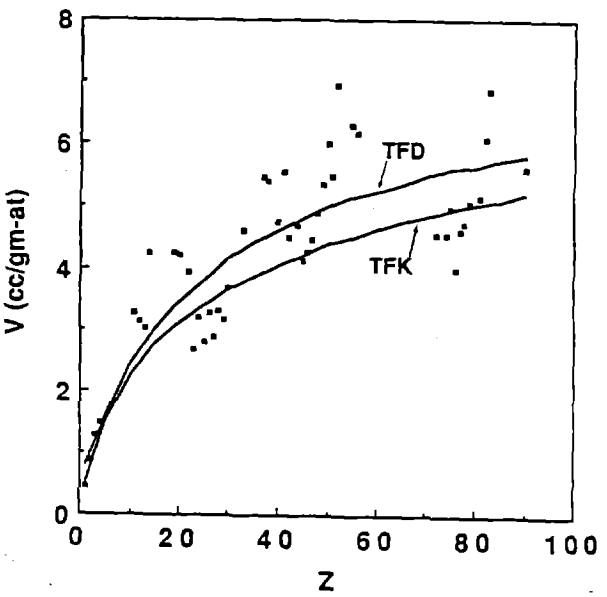

FIGURE 2
Comparison of the atomic volumes of the elements at 10 Mbar with the TFD and TFK theories.

The rapid smoothing of the atomic volume happens because the elements with the largest volumes are also the most compressible. This correlation is most obvious for the metals in a plot of bulk modulus vs. the interstitial electron gas radius r_s, shown in Fig. 3.[4]

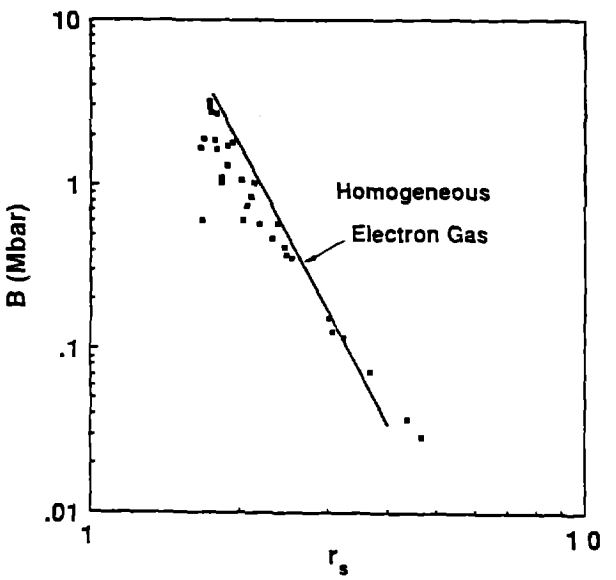

FIGURE 3
Correlation of the measured bulk modulus of some metallic elements with the calculated interstitial electron gas parameter. The theoretical homogeneous electron gas curve is shown.

Thus the behavior of the metallic elements is close to that of the homogeneous electron gas, and under compression elements with large r_s values will move up the curve toward those with smaller r_s values.

The cohesive energy is another natural descriptive parameter for the elements. It also shows periodic behavior, but with much wider swings than the atomic volume. The cohesive energy, however, is not completely independent from V_o and B_o. On a plot of energy vs. density, E_{coh} is the intercept at $\rho = 0$ and B_o is proportional to the curvature at $\rho = \rho_o$. The larger the curvature and B_o, the higher the value of E_{coh}. These two parameters can be formally related by the equation $E_{coh} = .5\ A(C_o/S)^2$, where A is the atomic weight, C_o is the sound speed, and S is the slope of the shock velocity-particle velocity curve.[5] This is shown in Fig. 4, with a moderately good correlation.

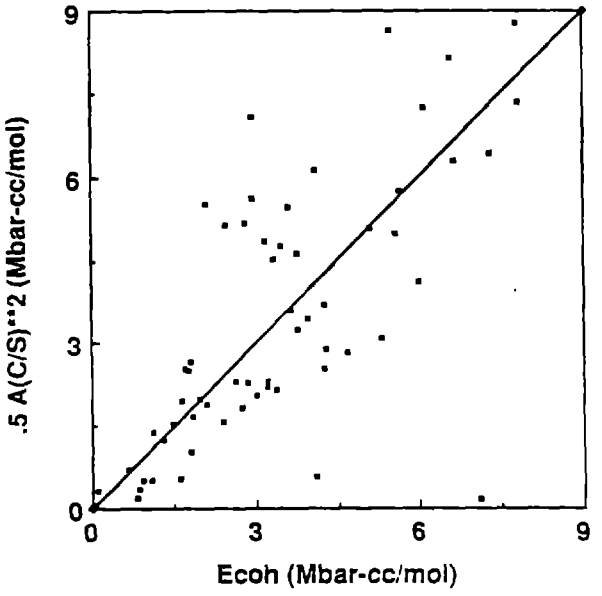

FIGURE 4
Correlation of the cohesive energy with the bulk modulus ($B_0 = C_0^2/V_0$) according to the McQueen-Marsh equation. The line indicates agreement with the equation.

3. CRYSTAL STRUCTURE

A more difficult property to explain is the crystal structure. The stable structure of an element will depend on subtle details of the interatomic potential, because it is competing with other structures of nearly equal free energy. Nevertheless, it is remarkable how many of the elements have the simple dense-packed structures fcc, hcp, or bcc.[6] This stability reflects the geometric packing imposed by a smooth repulsive interatomic potential which favors fcc or hcp, or alternatively, the Madelung electrostatic energy which favors bcc.

In Fig. 5 I show the crystal structures of the elements at 1 bar. Most of the metallic elements are dense-packed, while the non-metallic elements of the upper right corner of the table are covalent and have more open structures. As pressure increases, covalent bonds are destabilized and the elements of the upper right corner evolve toward dense-packed structures. At the same time, the metals of

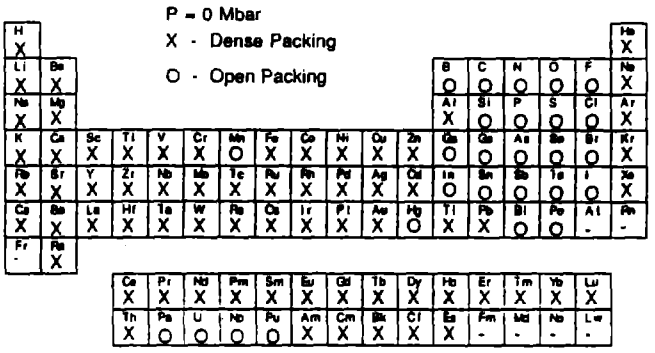

FIGURE 5
The observed crystal structures of the elements at 1 bar.

the left side of the table, including the Lanthanides and Actinides, show an s - d or s - f electron transfer which stabilizes non-close-packed structures such as tetragonal Cs IV and orthorhombic α-U. At 1 Mbar, the pattern of structures from measurement, theoretical calculation, and guesswork is shown in Fig. 6, where these two "waves" of structural change are moving across the table. There is some evidence that at still higher pressures where the s - d transfer is complete, the structures will revert to dense-packing.[7] Whether band-crossings in the ultrahigh pressure region will once again stabilize open structures is unknown.

Temperature also has an effect on crystal structure, the most common being the appearance

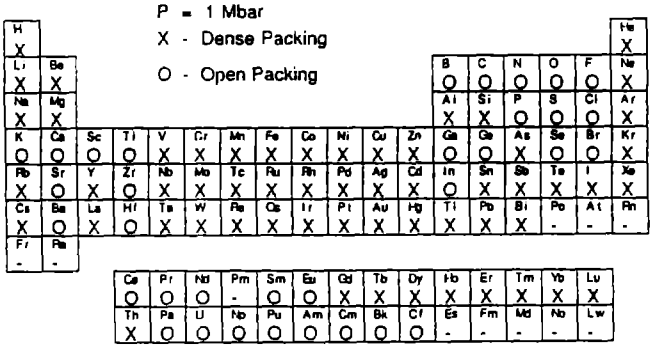

FIGURE 6
The observed and theoretically predicted crystal structures of the elements at 1 Mbar.

of a bcc phase a short distance before melting. This is an entropy effect which can be understood in terms of repulsive potentials of variable hardness.[8] For inverse-power potentials of the form $u(r) = 1/r^n$, the bcc phase will have a range of stability for all $n < 7.6$. Using the relation $\gamma = (n + 2)/6$, where γ is the Grüneisen parameter, for the inverse-power harmonic lattices, we note that a bcc phase is expected to appear in close-packed solids for $\gamma < 1.6$. This rule holds very approximately for close-packed metals, but since bcc can be stabilized by band structure energy as well as by high temperatures, the problem of computing the stability of bcc is complex, and there does not yet exist a theoretical model which explains the observations quantitatively.

4. MELTING AND VAPORIZATION

At still higher temperatures, the liquid is the stable phase and the systematics of melting are of great interest. Like the other parameters discussed here, the melting temperature exhibits periodicity. It is well-correlated with the cohesive energy, as shown in Fig. 7. This correlation can be explained in terms of a model of particles interacting according to simple repulsive potentials in an attractive mean field. For hard spheres or inverse-power potentials the relation between the melting temperature and the strength of the mean field (cohesive energy) is linear, and the theoretical slopes are shown in Fig. 7. It can be seen that the theory provides an approximate agreement with experiment.

Shock-wave experiments and theoretical calculations have been providing new data on melting in the megabar pressure region, and it is now possible to consider the evolution of the melting curves of the elements to very high pressures.[9-12] This is shown in Fig. 8.

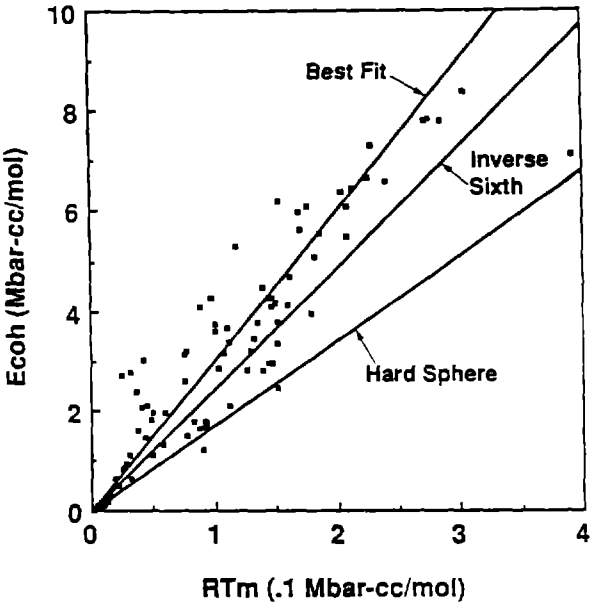

FIGURE 7
Correlation of the cohesive energy with the melting temperature. The hard sphere and inverse sixth mean-field theory predictions are shown in comparison with the best fit through the data.

These curves indicate a remarkable increase in melting temperature of the rare gases with pressure. As seen in Fig. 8, the melting temperature of Ar crosses those of Fe, Al, and Xe by 1 Mbar. It appears that at pressures above 1 Mbar, elements like Ar and Ne may have the highest melting temperatures of any element.

At extreme pressures, atoms are completely pressure-ionized and their melting curves will approach those of the one-component plasma with nuclear charge Z. These melting curves will then form a regular monotonic series with temperatures increasing with Z. Unlike the atomic volumes, this is an effect which becomes visible only at pressures and temperatures far beyond the experimental range.

At low pressures beyond the melting point we find the liquid-vapor region and the critical point. The critical points of about 20 elements have now been measured, and it is useful to examine these data. A good theo-

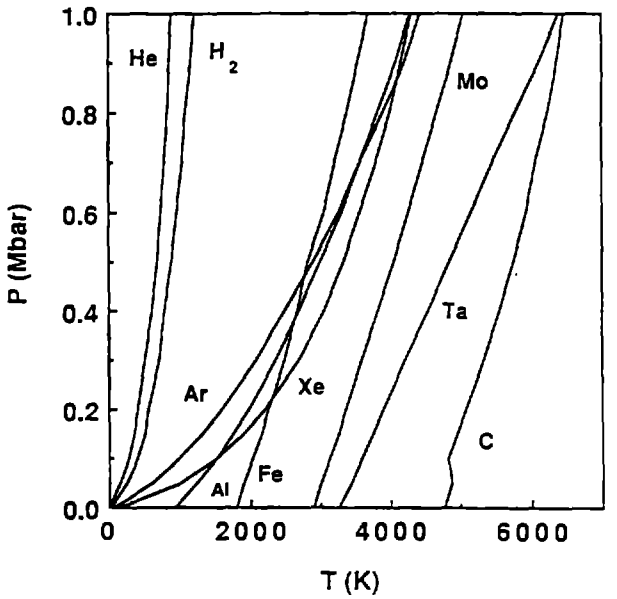

FIGURE 8
Measured and theoretically calculated melting curves to 1 Mbar.

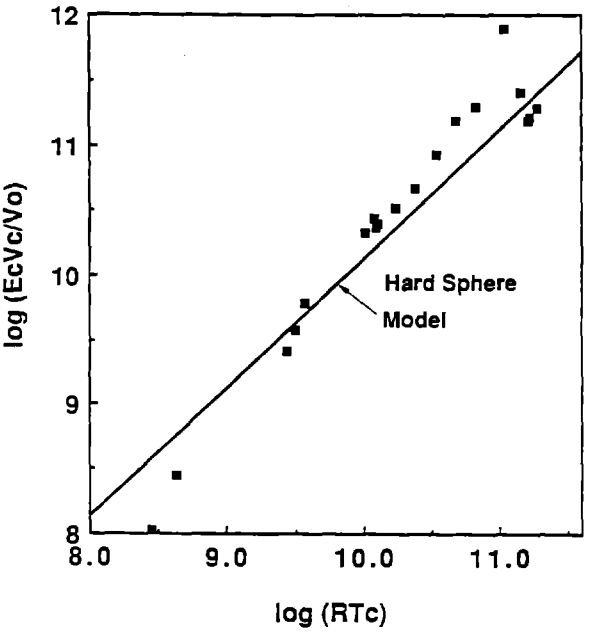

FIGURE 9
Correlation of the cohesive energy with the critical temperature, according to the hard sphere theory.

retical correlation can be taken from the hard-sphere theory[13] of the critical point, in which the two parameters are related according to the equation $RT_c = 0.7232 E_{coh} V_o / V_c$. This is plotted in Fig. 9, and is found to be a good fit to the collected critical point data.

Among the metals, only the critical points of K, Rb, Cs, and Hg have been measured.[14] For high cohesive energy metals like Fe and W, it is clear that dynamic methods will be needed to measure the critical parameters. This is a significant challenge to experimental technique. From correlations such as that shown in Fig. 9, we can estimate the highest critical temperatures and pressures to be near 10000 K and 10 kbar.[15]

5. CORRESPONDING STATES

The principle of corresponding states,[16] which relates the equation of state of one substance to another when both share a common two-parameter functional form of the interaction potential, is expected to hold for elements belonging to the same column in the periodic table. This has been shown to be true for the rare gases at low pressure,[17] and other groups such as the alkali metals and the Group IV elements show phase diagrams which are very similar to one another, in agreement with this principle. However, the very high pressures now attainable in the diamond anvil cell have revealed large deviations from corresponding states in the case of the rare gases, as shown in Fig. 10. Here Ne, Ar, and Xe are compared in reduced coordinates. Ne is expected to deviate from the others because of quantum effects, but the deviation of Ar from Xe is the result of the "softening" of Xe as it approaches metallization.[18] This also accounts for the crossing of the Ar and Xe melting curves at high pressure shown in Fig. 8. Hence it can be asserted that corresponding states can only work in restricted regions of pressure and temperature where the details of the electron band structure are not important.

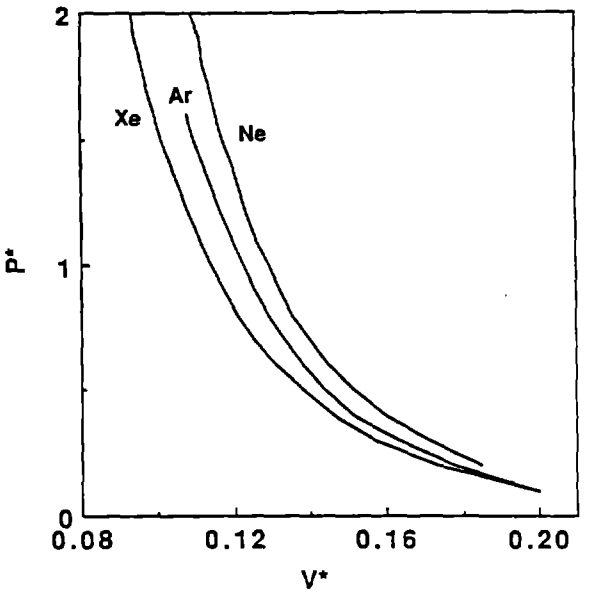

FIGURE 10
Comparison of the Ne, Ar, and Xe equations of state in scaled variables ($P^* = P/P_c$; $V^* = V/V_c$).

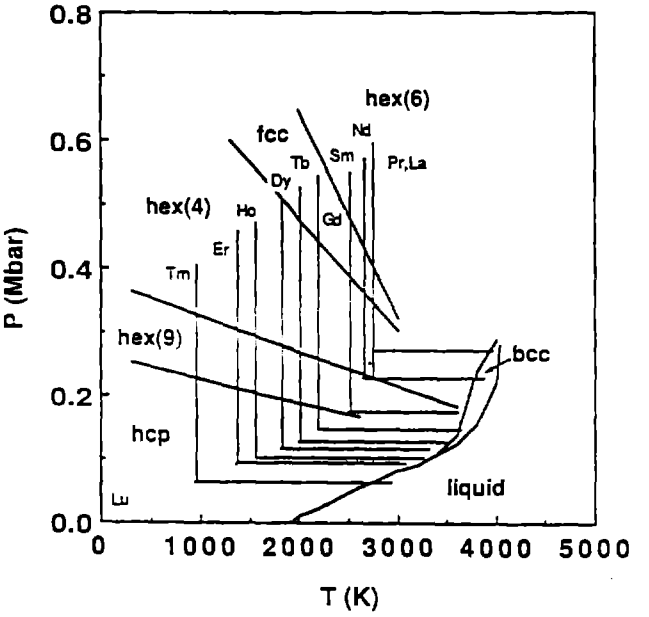

FIGURE 11
The generalized Lathenide phase diagram.

It is possible to consider "generalized" corresponding states principles where three or more parameters determine the equation of state and phase diagram. A well-known example is the phase diagram of the trivalent Lanthanide metals.[19] The individual Lanthanide diagrams can be superimposed to produce a single general diagram showing all of the phases characteristic of the Lanthanides, as shown in Fig. 11. It is significant that a similar diagram for the Actinides cannot be constructed, in part because of strong relativistic effects.

6. CONCLUSION

As we obtain more data on the solid and liquid elements, we discover more correlations among measured properties which bring out new relationships among the elements. However, we also discover exceptions to the rules which emphasize the uniqueness of each element. The rich structure of the Periodic Table is revealed in the balancing of these two tendencies.

ACKNOWLEDGEMENT

I thank R. Grover for many useful discussions.

REFERENCES

1. J. Emsley, Interdiscip. Sci. Rev. 12, (1987) 23.

2. C. N. Singman, J. Chem. Educ. 61, (1984) 137.

3. L. V. Al'tshuler and A. A. Bakanova, Usp. Fiz. Nauk 96, (1968) 193 [Sov. Phys. Usp. 11, (1969) 678].

4. V. L. Moruzzi, J. Janak, and A. R. Williams, Calculated Electronic Properties of Metals (Pergamon, New York, 1978).

5. R. G. McQueen and S. P. Marsh, J. Appl. Phys. 33, (1962) 654.

6. J. Donohue, The Structures of the Elements (Wiley, New York, 1974).

7. A. K. McMahan, Phys. Rev. B 29, (1984) 5982.

8. W. G. Hoover, D. A. Young, and R. Grover, J. Chem. Phys. 56, (1972) 2207.

9. D. A. Young and M. Ross, J. Chem. Phys. 74, (1981) 6950.

10. Q. Williams, R. Jeanloz, J. Bass, B. Svendsen, and T. J. Ahrens, Science 236, (1987) 181.

11. C-S. Zha, R. Boehler, D. A. Young, and M. Ross, J. Chem. Phys. 85, (1986) 1034.

12. R. S. Hixson, D. A. Boness, J. W. Shaner, and J. A. Moriarty, Phys. Rev. Lett. 62, (1989) 637.

13. D. A. Young and B. J. Alder, Phys. Rev. A 3, (1971) 364.

14. F. Hensel, S. Jüngst, B. Knuth, H. Uchtmann, and M. Yao, Physica 139&140B, (1986) 90.

15. D. A. Young, Lawrence Livermore Laboratory Report UCRL-52352, Nov. 1977 (unpublished).

16. J. O. Hirschfelder, C. F. Curtiss, and R. B. Bird, Molecular Theory of Gases and Liquids (Wiley, New York, 1964) Chap. 4.

17. R. K. Crawford, in: Rare Gas Solids, Vol. 2, eds. M. L. Klein and J. A. Venables (Academic, London, 1977) Chap. 11.

18. R. Reichlin, K. E. Brister, A. K. McMahan, M. Ross, S. Martin, Y. K. Vohra, and A. L. Ruoff, Phys. Rev. Lett. 62, (1989) 669.

19. B. Johansson and A. Rosengren, Phys. Rev. B 11, (1975) 2836.